Physica Scripta

PAPER

Tritium in plasma-facing components of JET with the ITER-Like-Wall

E Pajuste[1,2], A S Teimane[1], G Kizane[1], L Avotina[1], M Halitovs[1], A Lescinskis[1], A Vitins[1], P Kalnina[1], E Lagzdina[1], R J Zabolockis[1] JET Contributors[3,4]

[1] Institute of Chemical Physics, University of Latvia, 1 Jelgavas street, Riga, Latvia
[2] Faculty of Chemistry, University of Latvia, 1 Jelgavas Street, Riga, Latvia
[3] EUROfusion Consortium, JET, Culham Science Centre, Abingdon, OX14 3DB, United kingdom
[4] See the author list of E Joffrin *et al* 2019 *Nucl. Fusion*, **59**, 112021.

E-mail: elina.pajuste@lu.lv

Keywords: joint European torus, ITER like wall, tritium, plasma facing components

OPEN ACCESS

RECEIVED
20 June 2021

REVISED
10 September 2021

ACCEPTED FOR PUBLICATION
24 September 2021

PUBLISHED
1 November 2021

Abstract

The ITER-Like-Wall project has been carried out at the Joint European Torus (JET) to test plasma facing materials relevant to ITER. Materials being tested include both bulk metals (Be and W) and coatings. Tritium accumulation mechanisms and release properties depend both on the wall components, their location in the vacuum vessel, conditions of exposure to plasma and to the material itself. In this study, bulk beryllium limiter tiles, plasma-facing beryllium coated Inconel components from the main chamber, bulk tungsten and tungsten coated carbon fibre composite divertor tiles were analysed. A range of methods have been developed and applied in order to obtain a comprehensive overview on tritium retention and behaviour in different materials of plasma facing components (PFCs). Tritium content and chemical state were studied by the means of chemical or electrochemical dissolution methods and thermal desorption spectroscopy. Tritium distribution in the vacuum vessel and factors affecting its accumulation have been assessed and discussed.

1. Introduction

Tokamak type reactors are the dominant experimental technique for studying nuclear fusion. One of the largest present-day tokamak device, The Joint European Torus (JET), located near Oxford in United Kingdom, was put into operation in 1983. Currently, the International Thermonuclear Experimental Reactor ITER is under construction in Cadarache, Southern France. ITER-Like-Wall project has been carried out at the JET in order to study the compatibility of plasma operation with the plasma facing materials relevant to ITER and estimate fuel retention and material migration [1]. Since 2011, three series of campaigns had taken place: ILW1 (2011–2012), ILW2 (2013–2014) and ILW3 (2015–2016). During the shutdowns wall components had been retrieved for *ex situ* measurements. In this study, tritium concentration in different materials of the vacuum vessel has been measured, tritium accumulation pattern in the samples exposed for the separate ILW campaigns and for all the period assessed.

1.1. Plasma facing components in JET ITER like wall

Materials being tested include bulk beryllium, bulk tungsten, beryllium coated Inconel and tungsten coated carbon fibre composite. Positions of each material type in the vacuum vessel are illustrated in figure 1.

Plasma facing materials possess very different properties and, therefore, each requires a different approach for the measurements of tritium trapped in the surface, sub-surface and the bulk.

Beryllium's advantages as a plasma facing material are its low Z, good thermal conductivity, and high oxygen gettering characteristics. It has been tested as a plasma facing material also in earlier experiments both in JET, with its first introduction in 1989, as well as a smaller early period tokamaks such as UNITOR and ISX-B [2]. The main drawback of the use of beryllium is its high toxicity. A comprehensive overview on beryllium as PFM is provided by Temmerman *et al* [3].

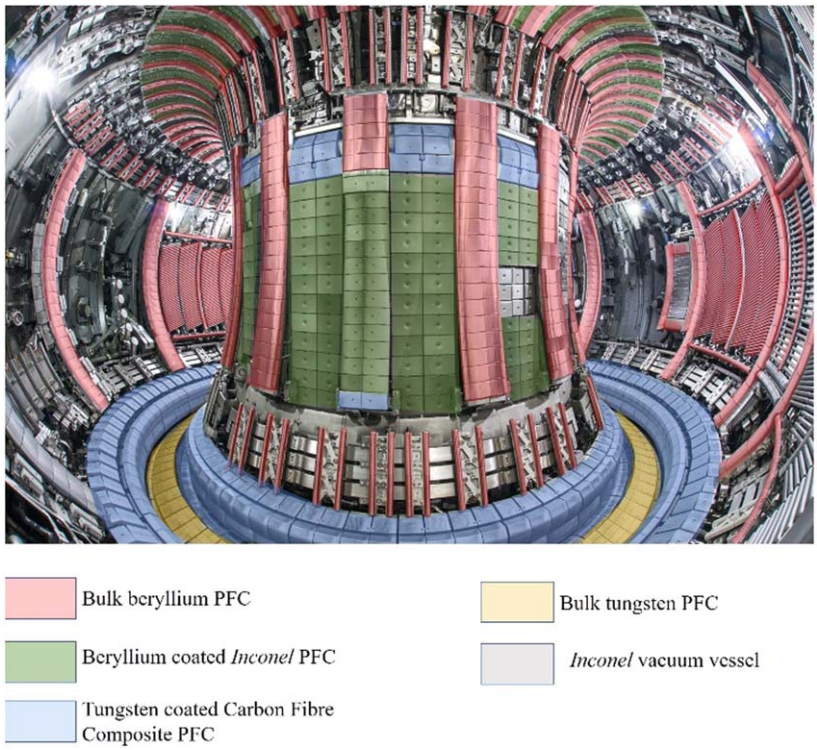

Figure 1. Plasma facing materials in JET ITER-Like-Wall.

Tungsten has good thermal properties with a very high melting point, however, it can cause deleterious radiation losses if entering the plasma. Therefore, tungsten and its coatings are used only in the vessel location where high thermal loads are expected.

The use of carbon based materials has a long history since development of nuclear fission reactors - carbon has very good thermal properties, high melting point and low Z [4]. However, there is a limitation due to high fuel retention that has been observed during full carbon wall campaigns at JET [5]. Fuel retention in CFC is related to intense dust generation [5] and hydrogen chemical affinity to carbon [6]; both lead to the intense tritium co-deposition.

Inconel is a nickel-based alloy with following chemical composition: $Ni_{53}Fe_{19}Cr_{19}NbMoTi$. It has been chosen as a vessel construction material due to its good oxidation and corrosion resistance, as well as good mechanical and thermal properties. It is also used as a substrate for beryllium coating due to the matching thermal expansion coefficients ($11.4{\cdot}10^{-6}\,K^{-1}$ and $11.2{\cdot}10^{-6}\,K^{-1}$ for beryllium and Inconel, respectively).

1.2. Tritium sources in JET

Up to 2021, no tritium introduction was done within the ITER-Like-Wall campaign. Nevertheless, there are several other possible sources of tritium:

- in-vessel tritium inventory remaining from previous D–T campaigns;
- energetic tritium ion production as a result of D–D reaction;
- tritium production in neutron-induced transmutation of beryllium (can be considered negligible in these results as we report in the following).

Tritium has been introduced in the vacuum vessel in three campaigns: Preliminary Tritium Experiment (PTE) in 1991 [7] the first Deuterium-Tritium Experiment (DTE1) in 1997 [8, 9] and the Trace Tritium Experiment (TTE) in 2003 [10]. In total 35.39 g ($5\cdot10^{24}$ atoms or 9 PBq) of tritium have been introduced (5 mg —PTE, 35 g—DTE1 and 380 mg—TTE) [11]. The highest contribution was the DTE1 experiment with the largest tritium amount being introduced into the torus, mainly by gas puffing. DTE1 was followed by clean-up period of about 3 months in order to remove tritium by running discharges in H, D or Glow Discharge cleaning mode, baking and venting [5]. Moreover, most of remained tritium must be removed together with the extracted

CFC tiles during the exchange to metallic wall components. Additionally, tritium decay also must be taken into account as its half-life is comparably short – 12.32 years [12].

Tritium produced as a result of D—D reaction (1) has its own kinetic energy of 1.01 MeV [11] that leads to its ability to implant into the material.

$$^{2}_{1}\mathrm{H(D)} + {}^{2}_{1}\mathrm{H(D)} \rightarrow {}^{3}_{1}\mathrm{H(T)} + {}^{1}_{1}\mathrm{H(H)} + 4.03\ \mathrm{MeV} \quad (1)$$

Both gas puffed and D—D tritium ion behaviour in plasma has been studied in Tokamak Fusion Test Reactor TFTR [13] where both D—D and D—T fusion reactions have been achieved [14, 15].

Neutron induced transmutation of beryllium will have a significant role in the future fusion devices such as ITER. Beryllium neutron interactions have been studied widely, especially, regarding its planned use as a neutron multiplier in tritium breeding blanket [16–18]. An example of Be transmutation chain where tritium can be produced is given in the following reactions 2–4 [19].

$$^{9}_{4}\mathrm{Be} + n(\mathrm{fast}) \rightarrow {}^{10}_{4}\mathrm{Be}^{*} \rightarrow {}^{4}_{2}\mathrm{He} + {}^{6}_{2}\mathrm{He} - 0.64\ \mathrm{MeV} \quad (2)$$

$$^{6}_{2}\mathrm{He} \rightarrow {}^{6}_{3}\mathrm{Li} + \beta^{-}(0.8\ s) \quad (3)$$

$$^{6}_{3}\mathrm{Li} + n(\mathrm{thermal}) \rightarrow {}^{3}_{1}\mathrm{H(T)} + {}^{4}_{2}\mathrm{He} + 4.78\ \mathrm{MeV} \quad (4)$$

Overall neutron yield in ILW campaign was very low and its contribution to tritium generation can be considered as insignificant. According to Fonnesu *et al* [20], neutron budget in the ILW1, ILW2 and ILW3 was $7.71{\cdot}10^{18}$, $1.85{\cdot}10^{18}$ and $2.15{\cdot}10^{19}$, respectively (or ~$3.5–10{\cdot}10^{16}$ m^{-2} if vessel inner wall surface of 220 m^2 is used in calculations [21]). According to the data from fast neutron (> 1MeV) irradiation experiments of beryllium at High Flux Reactor in Petten [22], irradiation to neutron flux up to $2{\cdot}10^{26}$ m^{-2} generates about 640 appm or $4.3{\cdot}10^{19}$ atoms of tritium per gram of beryllium [18]. In case of neutron fluxes at JET, concentration of tritium would be ~10^{10} atoms that is near or below detection limit of measurement devices.

1.3. Tritium interaction with plasma facing materials, retention mechanisms

Co-deposition with eroded materials and physical diffusion into the bulk of wall material are being considered as the main tritium accumulation mechanisms in the first wall materials. Co-deposited tritium mainly retains in near surface of the plasma facing material, however tritium as a hydrogen isotope is very mobile due to its small size and might diffuse much deeper into the bulk. Energetic ion implantation into the material has been also widely studied [23].

1.4. Tritium measurement methods

There are various approaches for tritium measurements depending on the material and required information.

Thermal Desorption spectrometry TDS is a standard method providing information on total amount of tritium, estimations of detrapping energies and diffusion is also possible. TDS can be performed both in a purge gas and vacuum, tritium measurement—by the means of mass spectrometry or radiometric methods. TDS has been applied both for deuterium and tritium measurements [24–26], however, tritium concentration in JET samples is very low and high sensitivity detection method is required.

The full combustion method followed by tritium measurements with liquid scintillation can be applied to all combustible materials, such as carbon and metals. This method has been originally developed by Vance *et al* [27] and has been applied to various JET materials [28, 29].

X-ray photoelectron spectrometry [30] has a high resolution (nm), however it is limited only to near surface tritium measurement: 3 μm and 0.3 μm for Be and W, respectively. Method has been applied to the JET vacuum vessel tiles retrieved during ILW shutdowns [29, 31].

Imaging plate technique is based on tritium beta radiation interaction with radiosensitive material. Due to small beta radiation range in solid samples method gives information only on the near surface tritium [32].

Glow discharge optical emission spectroscopy (GD-OES) is based on simultaneous surface etching with Ar plasma and optical stimulation of the eroded material. Currently, this method has been demonstrated on stable hydrogen isotopes H and D, only [33].

Chemical and electrochemical etching can be applied to the metallic samples and gives information both on total tritium amount and its depth profile [34]

2. Experimental

2.1. Materials

In this study, tiles retrieved during ILW1, ILW2 and ILW3 shutdowns have been analysed.

Those include bulk beryllium tiles from inner, outer walls and upper part of the vessel, beryllium coated Inconel from inner wall and bulk tungsten and tungsten coated CFC tiles from three divertor positions. Some

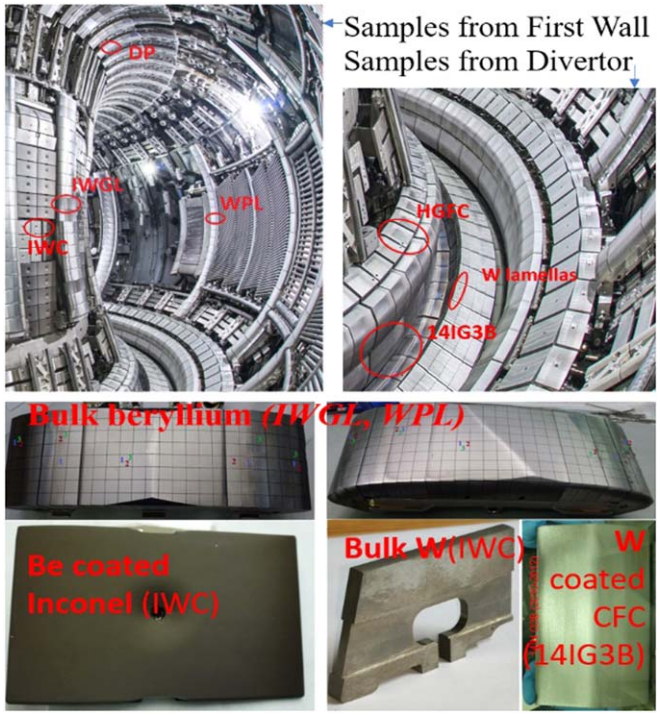

Figure 2. Position of analysed material in the vacuum vessel.

beryllium samples have been in the vacuum vessel throughout all 3 campaigns. Locations of the studied samples and their photographs are provided in figure 2.

2.2. Methods

Dissolution/etching method is based on the simultaneous etching of the metal surface and measurements of the released tritium. Beryllium can be etched chemically in acid solutions, whereas for tungsten and Inconel electrochemistry must be applied due either to their low reactivity with chemical etchants or formation of complex mixtures of the reaction products. Detailed description of the methods for Be and W is given in [34]. In case of Be coated Inconel combination of chemical (beryllium) and electrochemical (Inconel) etching has been applied that gives opportunity to measure separately tritium accumulated in the coating and substrate. Released tritium in Ar purge gas (T_2, HT, DT) has been measured by proportional counter with an operating volume of 300 cm^3 and a tritium monitor TEM 2102A (Mab Solutions GmbH), whereas tritium remaining in solution (HTO, DTO, T^+) with liquid scintillation counter TRi-Carb 2910TR (PerkinElmer, Inc.).

Full combustion method has been applied to tungsten coated CFC samples. Released tritium oxidized into water (HTO, DTO) and measured by liquid scintillation.

Thermal desorption of tritium was performed in a flow of He+0.1% H_2 purge gas. A sample is placed and heated in a quartz tube with two compartments—one for the sample and one for a bed of granulated zinc. A quartz cap of the tube had a thermocouple channel. The zinc bed is used to convert tritiated water to molecular gaseous tritium (HT, DT, and traces of T_2). The temperatures of the sample, the zinc bed and the cold trap were continuously measured. The tritium activity in the purge gas was continuously monitored using a proportional counter (similar model as described above). Heating rate of 5 K has been used with a maximum temperature 1305 K.

Tritium decay has been considered and all the measurement data recalculated as per day of the retrieval of the material from the vacuum vessel.

3. Results and discussion

Total amount of tritium measured by different methods, its surface and bulk distribution, retention behaviour in different plasma facing materials exposed to D—D plasma during ILW have been discussed in this manuscript.

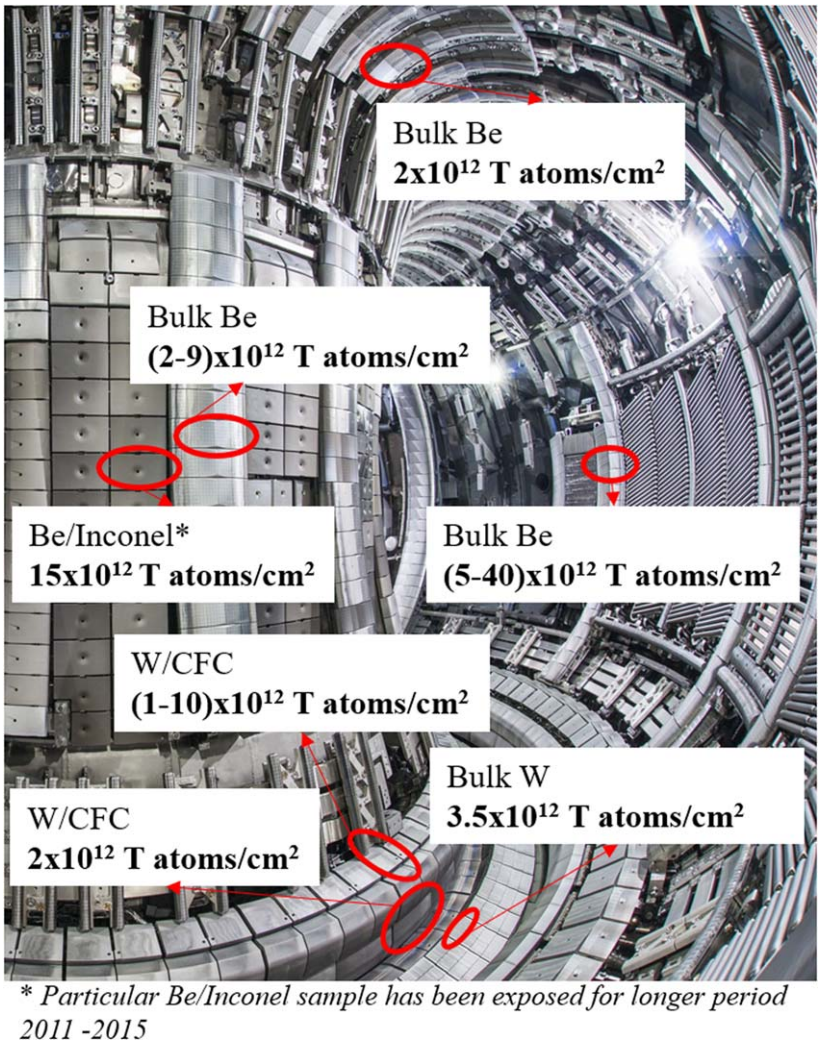

Figure 3. Tritium concentration in different locations of the vacuum vessel.

Table 1. Tritium concentration in different locations in vacuum vessel after ILW1.

Location	Material	T atoms $cm^{-2} \times 10^{12}$
Upper part	Bulk Be	2.8 (one sample)
Inner wall	Bulk Be	3–9
Inner wall	Be/Inconel	15 (one sample)
Outer wall	Bulk Be	4–40
Inner divertor (tile 3)	W/CFC	2
Inner divertor (HGFC)	W/CFC	1–10
Divertor floor	Bulk W	3.5 (one sample)

3.1. Tritium distribution within vacuum vessel

Tritium concentration as atoms per square centimetres of plasma facing surface had been assessed for all materials from different location on the vacuum vessel. Data obtained for samples retrieved in 2012 are compared in this chapter (table 1, figure 3). Tritium concentration has been found to be in range from $1{\cdot}10^{12}$ to $4{\cdot}10^{13}$ atoms cm^{-2} with its highest concentration in outer wall bulk beryllium limiter tiles. In contrast to deuterium data, no increase of tritium concentration was observed in the deposition zones of divertor, where its concentration was in range 10^{12} to 10^{13} atoms/cm^2. According to Widdowson *et al* [35] deuterium concentration in inner divertor and inner wall limiter tiles ratio were about 10:1 ($17{\cdot}10^{22}$ and $1.4{\cdot}10^{22}$ D atoms, respectively), whereas for tritium it is ~1:1 ($5{\cdot}10^{12}$ and$\cdot 10^{12}$ T atoms, respectively). These results indicate that co-deposition is not the main tritium source in wall materials. A detailed comparison of tritium data with deuterium in bulk beryllium tiles and differences of ILW series has been published elsewhere [36].

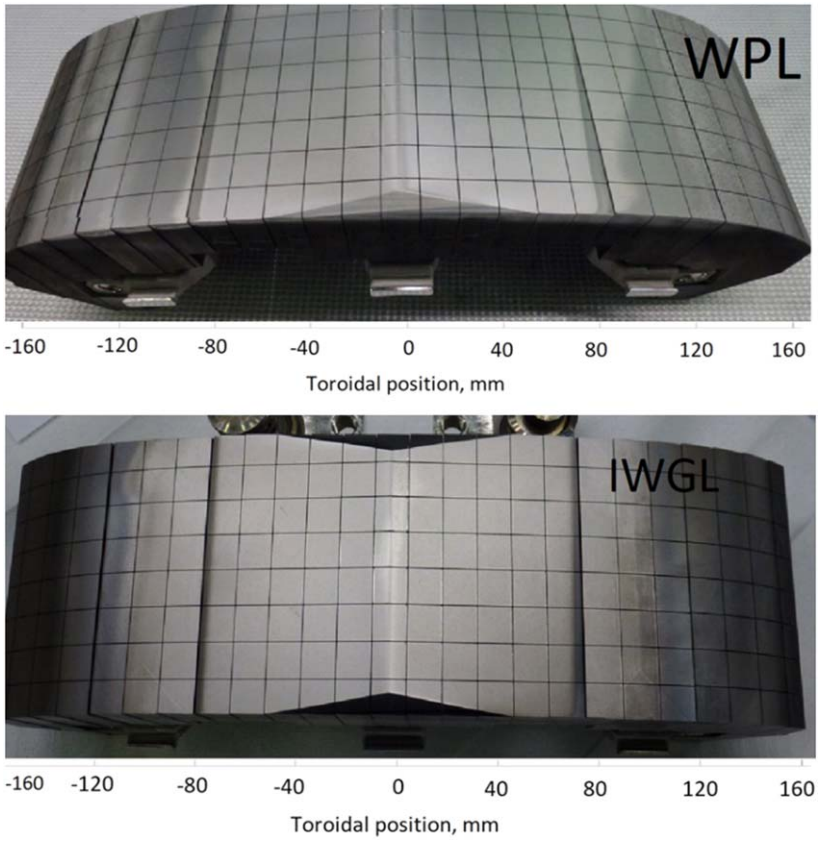

Figure 4. Beryllium tiles and toroidal scale.

Table 2. Tritium concentration at particular positions in vacuum vessel in tiles exposed to each campaign [36] and tiles exposed throughout all campaigns.

Position, mm	T atoms $cm^{-2} \times 10^{12}$					%
	ILW1	ILW2	ILW3	Sum	1–3	
Outer wall tile WPL						
−146	15	18	33	66	39	59
−33	16	22	39	77	81	105
98	4	21	11	35	15	42
146	3	2	4,6	10	2,5	25
Inner wall tile IWGL						
−145	2	0.5	0.3	3	2.4	77
−92	4	2	0.4	6	2.5	41
145	2.1	1.2	0.5	4	1.2	32

When comparing tritium accumulation in samples with similar toroidal locations (figure 4) from each campaign with those that remained in vacuum vessel throughout all 3 campaigns it was observed that accumulated tritium final amount is smaller than a sum of three separate campaigns.

These results demonstrates the simultaneous desorption process taking place in the vacuum vessel, mostly due to bake-outs, outgassing and erosion [37]. However, in separate samples exposed to all campaigns tritium concentration is higher that expected form the sum of the separate campaigns. That might be explained by the fact that samples are taken from slightly different poloidal positions. Comparison of the tritium concentration values recalculated to ILW3 retrieval day taking into account decay of tritium is given in the table 2.

4. Effects of deposition layer on tritium retention

The impact of the deposition layer thickness on tritium retention pattern has been assessed. Combination of scanning electron microscopy and energy dispersive x-ray spectroscopy was used for the layer analysis (Figure 5).

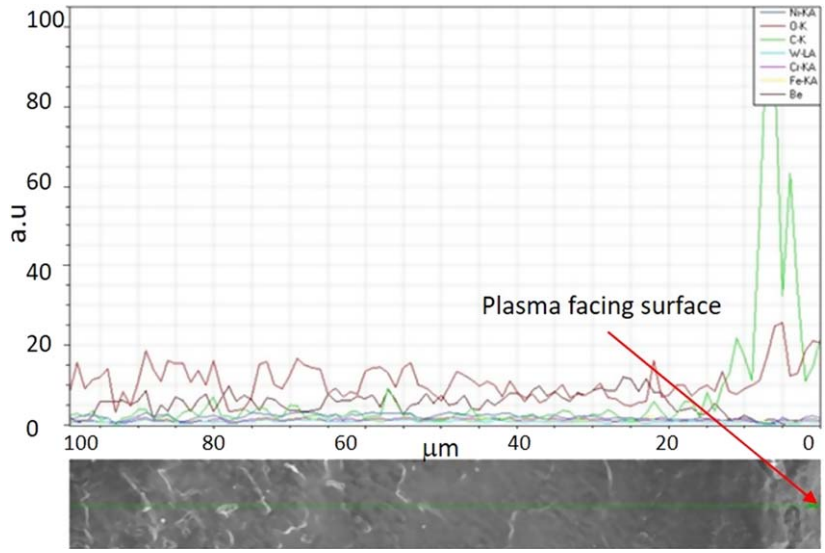

Figure 5. SEM/EDX combined line spectrum of sample from WPL tile.

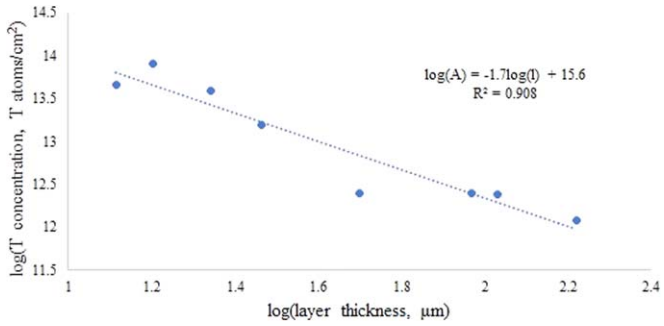

Figure 6. Correlation between deposition layer thickness and tritium concentration, where A = T atoms cm^{-2} and l = layer thickness in μm.

Table 3. Deposition layer thickness and tritium concentration in Be samples exposed during all three campaigns.

Position, mm	Layer thickness, μm	T atoms $cm^{-2} \times 10^{12}$
	Outer wall	
−146	22 ± 1	39.1 ± 0.6
−96	13 ± 3	46.2 ± 0.6
−33	16 ± 1	80.5 ± 1.0
98	29 ± 7	15.5 ± 0.3
146	50 ± 6	2.46 ± 0.06
	Inner wall	
−145	107 ± 5	2.43 ± 0.05
−92	93 ± 3	2.53 ± 0.06
145	166 ± 4	1.20 ± 0.01

For the determination of the carbon deposit layer, SEM/EDX line spectrum has been acquired and measured. In figure 5 - line spectrum of the beryllium sample cross section.

Three distinct areas can be identified—deposition layer mainly consisting of carbon at the plasma facing, beryllium roughening and oxidation in the middle and intact beryllium deeper in the bulk. Thickness of the deposition layer has been measured for the selected samples prior to tritium measurement and correlation assessed (Table 3).

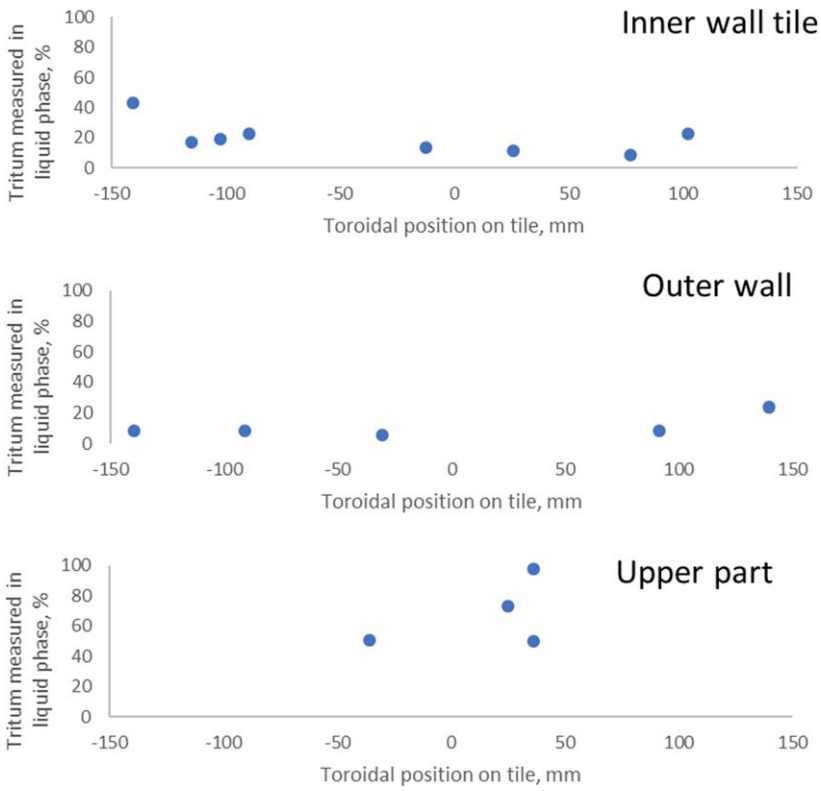

Figure 7. Tritium measured in the liquid phase (chemically bonded) in Be tiles after all three campaigns.

A linear correlation can be seen when looking at acquired data in logarithmic scale ($R^2 = 0.908$)—with increasing deposition layer the retained tritium concentration decreases (figure 6). A different trend can be observed for the samples retrieved from vacuum vessel than the ones acquired from artificial samples where tritium is co-deposited with carbon [38]. Multiple studies about the increase of deuterium retention by increasing the deposition layer can be found [38, 39] and many tend to assume similar trends for tritium, but current results show the opposite tendencies. However, these results suggest that high energy T implantation is dominant for tritium retention at the plasma facing surface instead of co-deposition as it is in the case of deuterium.

This is due to the D-D reaction during deuterium campaigns, in which high energy tritium ions are created. In further planned JET deuterium-tritium campaign and in ITER the dominant reaction will be D-T. However, also D-D reaction will be present, therefore high energy tritium ions must be considered. Deposits may have larger impact on tritium retention at grooves [40].

For tritium, main concerns associated with deposition layer formation are complicated desorption of tritium already accumulated. ITER bake-out temperature is planned to be 510 K, which might be enough for beryllium materials, but the desorbed deuterium and tritium might still be retained in the carbon deposit layer [41, 42].

4.1. Chemical state of tritium accumulated in Be

Dissolution method provides possibility to acquire information about possible chemical state of tritium [43]. During dissolution process of Be in sulphuric acid tritium trapped as interstitial atom or as a gaseous molecule (HT, DT or T_2) is released in gas phase and measured in the purge gas by the means of tritium monitor, whereas chemically bonded tritium remains in the liquid and is measured by liquid scintillation. Chemical reactions taking place during dissolution are as follows:

$$Be^0 + 2H^+ \rightarrow Be^{2+} + 2H^0 \quad (5)$$

$$H^0 + H^0 \rightarrow H_{2(g)} \quad (6)$$

$$H^0 + T^0_{(s)} \rightarrow HT_{(g)} \quad (7)$$

$$T_{2(s)} \rightarrow T_{2(g)} \quad (8)$$

$$T^{+}_{(s)} \rightarrow T^{+}_{(liq)} \quad (9)$$

By analysing the proportion of tritium measured in each phase, we can determine which type of retention—physical (interstitial or molecules) or chemical (bonded to oxygen or other impurities)—is dominant in different parts of the vacuum vessel. Most of the tritium quantified in liquid state can be found in samples from the upper part of the vacuum vessel where traces of melted and re-solidified beryllium were observed by microscopy (Figure 7).

These results demonstrated above correlate well with [1] where BeOD was detected only in the melted zones of JET tiles and, therefore, also BeOT formation could be expected where melting occurs.

According to the results on T retention in tungsten W and carbon C it has been found by Nobuta *et al* that T accumulated in C mostly forms chemical bonds (C-T). By storing these samples in vacuum for 40 days 16% of tritium is desorbed from carbon samples (mostly in the form of DT and T2). Tritium is mostly accumulated by physical trapping in W samples and after 18 days and 250 days 50% and up to 70% of the accumulated tritium had diffused out of the W samples, respectively [2].

It might be assumed that main contributing molecules of tritium chemical trapping are BeT and BeOxTy. In [3, 4] it has been emphasized that elevated temperatures are necessary to achieve tritium desorption from such trapping sites, but it is important to note that sputtering temperature for BeT is 440 K, which is 50 K lower than the planned tritium out-baking temperature at ITER.

Information of the tritium trapping mechanism is of great importance for detritiation planning, because high temperatures aimed at parts where potential chemical retention is present may lead to sputtering and therefore plasma contamination.

5. Conclusions

- Tritium concentration in the plasma facing components after D-D campaigns is in range from 0.3•1012 to 8·1013 atoms cm^{-2} with highest concentration in the outer wall beryllium limiters
- Tritium distribution pattern in the vacuum vessel and within single tiles is different from that for deuterium and is related to its accumulation as a energetic ion implantation in the materials in contrary to D main retention mechanisms - co-deposition. Energetic tritium ions are produced in D-D reaction, therefore, in DT campaigns its contribution will be considerably smaller.
- Tritium accumulation in the plasma facing materials is accompanied with the desorption and erosion processes that leads to the lower tritium concentration in materials exposed in vacuum vessel throughout all 3 campaigns

Acknowledgments

This work has been carried out within the framework of the EUROfusion Consortium and has received funding from the EURATOM research and training programme 2014–2018 and 2019–2020 under grant agreement No 633053. The views and opinions expressed herein do not necessarily reflect those of the European Commission.

Data availability statement

All data that support the findings of this study are included within the article (and any supplementary files).

ORCID iDs

E Pajuste https://orcid.org/0000-0003-1036-4679
G Kizane https://orcid.org/0000-0002-3206-5322
L Avotina https://orcid.org/0000-0001-5197-4196
A Vitins https://orcid.org/0000-0002-1010-1572
R J Zabolockis https://orcid.org/0000-0002-6654-9982

References

[1] Matthews G F *et al* 2007 Overview of the ITAB *Phys. Scr.* **T128** 137–43
[2] Federici Gianfranco *et al* 2016 Beryllium as a plasma facing material for near-term fusion devices *Reference Module in Materials Science and Materials Engineering.* (Germany: Elsevier) (https://doi.org/10.1016/B978-0-12-803581-8.09805-2)

[3] De Temmerman G et al 2021 Data on erosion and hydrogen fuel retention in Beryllium plasma-facing materials Nuclear Materials and Energy 27 100994
[4] Snead L L and Ferraris M 2012 4.18 - Carbon as a fusion plasma-facing material Comprehensive Nuclear Materials ed R J M Konings Editor (Oxford: Elsevier) pp 583–620
[5] Coad J P et al 2019 Material migration and fuel retention studies during the JET carbon divertor campaigns Fusion Eng. Des. 138 78–108
[6] Küppers J 1995 The hydrogen surface chemistry of carbon as a plasma facing material Surf. Sci. Rep. 22 249–321
[7] Team J E T 1992 Fusion energy production from a deuterium-tritium plasma in the JET tokamak Nucl. Fusion 32 187
[8] Keilhacker M et al 1999 High fusion performance from deuterium-tritium plasmas in JET Nucl. Fusion 39 209
[9] Jacquinot J et al 1999 Overview of ITER physics deuterium-tritium experiments in JET Nucl. Fusion 39 235
[10] Zastrow K D et al 2004 Tritium transport experiments on the JET tokamak Plasma Phys. Control. Fusion 46 B255
[11] Stork D et al 2005 Overview of transport, fast particle and heating and current drive physics using tritium in JET plasmas Nucl. Fusion 45 S181
[12] Purcell J E and Sheu C G 2015 Nuclear data sheets for A = 3 Nucl. Data Sheets 130 1–20
[13] Bell M G 2016 6 - The Tokamak Fusion Test Reactor, in Magnetic Fusion Energy ed G H Neilson (United States: Woodhead Publishing) pp 119–66
[14] Strachan J D et al 1994 Deuterium and tritium experiments on TFTR Plasma Phys. Control. Fusion 36 B3–15
[15] McGuire K M et al 1995 Review of deuterium–tritium results from the Tokamak fusion test reactor Phys. Plasmas 2 2176–88
[16] Fedorov A V et al 2013 Analysis of tritium retention in beryllium pebbles in EXOTIC, PBA and HIDOBE-01 experiments J. Nucl. Mater. 442 S472–7
[17] Pajuste E et al 2015 Behaviour of neutron irradiated beryllium during temperature excursions up to and beyond its melting temperature J. Nucl. Mater. 465 293–300
[18] Chakin V et al 2020 Tritium release and retention in beryllium pebbles irradiated up to 640 appm tritium and 6000 appm helium J. Nucl. Mater. 542 152521
[19] Evans J E 1956 Reaction Products in High NVT Irradiated Beryllium. (Idaho Falls, Idaho: Phillips Petroleum Co. Atomic Energy Div.) p. Medium: ED; Size: Pages 11
[20] Fonnesu N et al 2020 Shutdown dose rate studies for the DTE2 campaign at JET Fusion Eng. Des. 161 112009
[21] Rappé G H 1977 The J.E.T. (Joint European torus) vacuum vessel Revue de Physique Appliquee, 12 1735–41
[22] van Til S et al 2011 Evolution of beryllium pebbles (HIDOBE) in long term, high flux irradiation in the high flux reactor Fusion Eng. Des. 86 2258–61
[23] Tobita K et al 2003 First wall issues related with energetic particle deposition in a tokamak fusion power reactor Fusion Eng. Des. 65 561–8
[24] Baron-Wiechec A et al 2018 Thermal desorption spectrometry of beryllium plasma facing tiles exposed in the JET tokamak Fusion Eng. Des. 133 135–41
[25] Widdowson A et al 2020 Fuel inventory and material migration of JET main chamber plasma facing components compared over three operational periods Phys. Scr. T171 014051
[26] Vitiņš A et al 2013 Tritium release behavior of beryllium pebbles after neutron irradiation between 523 and 823 K J. Nucl. Mater. 442 s490–3
[27] Vance D E, Smith A M and Waterbury G R 1979 Quantitative determination of tritium Metals and Oxides (https://inis.iaea.org/collection/NCLCollectionStore/_Public/10/486/10486554.pdf)
[28] Ashikawa N et al 2020 Determination of retained tritium from ILW dust particles in JET Nuclear Materials and Energy 22 100673
[29] Pajuste E et al 2011 Structural changes and distribution of accumulated tritium in the carbon based JET tiles J. Nucl. Mater. 415 S765–8
[30] Hatano Y et al 2017 Tritium analysis of divertor tiles used in JET ITER-like wall campaigns by means of β-ray induced x-ray spectrometry Phys. Scr. 2017 014014
[31] Lee S E et al 2020 Tritium distribution analysis of Be limiter tiles from JET-ITER like wall campaigns using imaging plate technique and β-ray induced x-ray spectrometry Fusion Eng. Des. 160 111959
[32] Otsuka T and Tanabe T 2017 Application of a tritium imaging plate technique to depth profiling of hydrogen in metals and determination of hydrogen diffusion coefficients Mater. Trans. 58 1364–72
[33] Taylor C N and Shimada M 2017 Direct depth distribution measurement of deuterium in bulk tungsten exposed to high-flux plasma AIP Adv. 7 055305
[34] Pajuste E et al 2019 Novel method for determination of tritium depth profiles in metallic samples Nucl. Fusion 59 10
[35] Widdowson A et al 2017 Overview of fuel inventory in JET with the ITER-like wall Nucl. Fusion 57 086045
[36] Pajuste E et al 2021 Tritium retention in plasma facing materials of JET ITER-like-wall retrieved from the vacuum vessel in 2012 (ILW1), 2014 (ILW2) and 2016 (ILW3) Nuclear Materials and Energy 27 101001
[37] De Temmerman G et al 2017 Efficiency of thermal outgassing for tritium retention measurement and removal in ITER Nuclear Materials and Energy 12 267–72
[38] Hamaji Y et al 2015 Gaseous tritium uptake by C deposition layer on tungsten J. Nucl. Mater. 463 1017–20
[39] Tanabe T et al 2005 Comparison of tritium retention and carbon deposition in JET and JT-60U J. Nucl. Mater. 345 89–95
[40] Lee S E et al 2021 Global distribution of tritium in JET with the ITER-like wall Nuclear Materials and Energy 26 100930
[41] Nemanič V et al 2020 Deuterium inventory determination in beryllium and mixed beryllium-carbon layers doped with oxygen Fusion Eng. Des. 150 111365
[42] De Temmerman G et al 2009 Insight into the co-deposition of deuterium with beryllium: Influence of the deposition conditions on the deuterium retention and release J. Nucl. Mater. 390-391 564–7
[43] Pajuste E et al 2011 Tritium distribution and chemical forms in the irradiated beryllium pebbles before and after thermoannealing Fusion Eng. Des. 86 2125–8